Journal of Physics: Conference Series

Efficient reduction of four-loop massless propagators

To cite this article: T Ueda *et al* 2017 *J. Phys.: Conf. Ser.* **920** 012002

IOP Conf. Series: Journal of Physics: Conf. Series **920** (2017) 012002 doi:10.1088/1742-6596/920/1/012002

Efficient reduction of four-loop massless propagators

T Ueda[1], B Ruijl[1,2] and J A M Vermaseren[1]

[1] Nikhef Theory Group, Science Park 105, 1098 XG Amsterdam, The Netherlands
[2] Leiden Centre of Data Science, Leiden University, Niels Bohrweg 1, 2333 CA Leiden, The Netherlands

E-mail: `tueda@nikhef.nl`, `benrl@nikhef.nl`, `t68@nikhef.nl`

Abstract. In the light of precision measurements at the LHC experiments, theory predictions including higher-order corrections have become more important. We have developed a program `Forcer` dedicated to analytical evaluation of four-loop massless propagator-type Feynman integrals via parametric integration-by-parts reduction. Some recent physics results obtained by `Forcer` are discussed.

1. Introduction

In the last decade, much effort has been made on accurate theory predictions to meet requirements from precision experiments. Especially, precise QCD predictions are crucial for experiments at hadron colliders due to the strong interactions, hence theory calculations for higher-order radiative corrections in perturbative theory are mandatory to analyze a large amount of data from detectors.

A notoriously well-known example that slowly converges and hence requires higher-order calculations is the Higgs production cross section in the gluon-fusion channel $gg \to H$, which is the dominant channel in hadron colliders. In this channel, the next-leading order corrections in the strong coupling give a large contribution comparable to that from the leading order, thus in practice one has to use the next-to-next-to leading order (NNLO) prediction for any phenomenological studies. Recently, a more precise result for the total cross section including the next-to-next-to-next-to leading order (N^{3}LO) corrections in the heavy top-quark mass limit became available [1], which reduced the total uncertainty down to less than 10% for the LHC at 13 TeV.

One of the remaining sources of theory uncertainty for the total Higgs production cross section originates from the fact that parton distribution functions are extracted from experimental data via NNLO analysis while the partonic cross section is obtained up to the N^{3}LO. In order to improve this situation, one must know four-loop splitting functions, however, a direct computation of them sounds too challenging at present. A more promising approach in the near-to-mid term is to compute low-integer Mellin N-th moments of the splitting functions and estimate them via, e.g., Padé approximant. Indeed, such estimations were performed at the three-loop level [2, 3, 4] before the full N-dependence was computed [5, 6]. At the four-loop level, until recently, these computations had been done only up to $N = 4$ [7, 8, 9, 10].

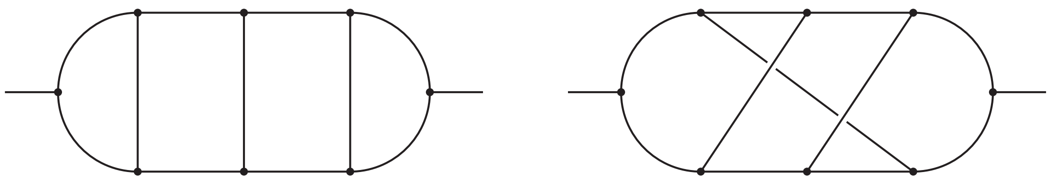

(a) ladder **(b)** non-planar (no1)

Figure 1. Two topologies out of 11 top-level topologies at the four-loop level.

Once N is fixed to an integer, such an N-th moment calculation reduces to evaluation of massless propagator-type Feynman integrals. Master integrals in this class of integrals are known at the four-loop level [11, 12]. The main obstacle for computing moments for higher N is, however, the reduction to the master integrals via integration-by-parts (IBP) identities [13, 14] within dimensional regularization [15, 16]. Although there are several generic IBP reduction methods available on the market — for example, Laporta's algorithm [17] (see [18, 19, 20, 21, 22, 23] for public implementations), Baikov's method [24, 25] and Lee's heuristic approach [26, 27] — it is still a tough problem to perform reductions needed for higher moments in a reasonable amount of computational time.

On the other hand, up to the three-loop level, it is known that many massless propagator-type integrals can be reduced into simpler ones by using the so-called triangle rule [13, 14, 28] constructed from the IBP identities and by performing one-loop massless integrations with G-functions [29, 14]. There are only two topologies that require manually solved IBP reduction rules [14]. In this way, the IBP reduction need not be performed when one arrives at integrals that can be expressed in terms of the gamma function. This approach was implemented in the `Mincer` program [30] written in `SCHOONSCHIP` [31] and later reprogrammed [32] in `FORM` [33, 34], which is highly efficient and has been used for many calculations including very high moments (e.g., [35, 36]).

The successful experience at the three-loop level suggests that if one could extend the `Mincer` program to the four-loop level then it might be more efficient than general IBP solvers for massless propagator-type integrals. This is a natural expectation because usually an algorithm with domain-specific knowledge has a better performance than a generic algorithm. This work aims to develop a new `FORM` package `Forcer` [37, 38, 39], which is, in a word, an extension of `Mincer` to the four-loop level, and push the limit of our capability for this class of integrals. Due to a high complexity of the program at the four-loop level, code generation must be as much automatized as possible. `Forcer` allows us to compute more high N moments of four-loop splitting functions and can be useful for other calculations (see [10] for a recent review on physics related to massless propagators).

2. Reduction of each topology by its substructure

Families of scalar Feynman integrals can be classified by their denominator structure or topologies of corresponding Feynman diagrams. In our case, all (squared) propagators appearing in the denominator are massless. Figure 1 shows example topologies at the four-loop level. Generic (top-level) topologies, consisting of three-point vertices, at this level have 11 internal lines. There are also 3 irreducible numerators, which cannot be expressed in terms of propagators, and hence they are characterized by 14 parameters (called as indices).

As seen in the `Mincer` approach, some substructures found in topologies lead to reduction rules of integrals belonging to a topology into ones in simpler topologies.

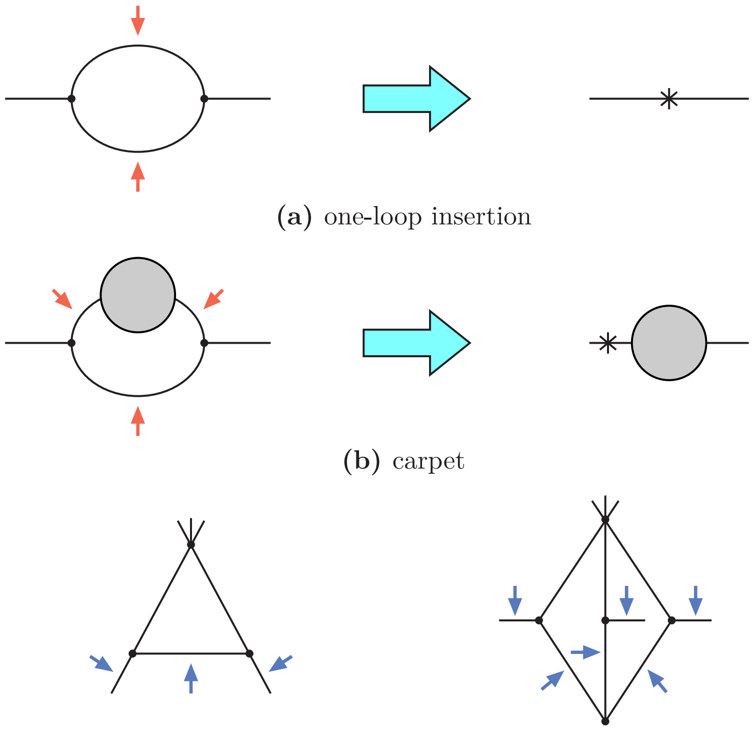

(a) one-loop insertion

(b) carpet

(c) triangle **(d)** diamond

Figure 2. Substructures of topologies that give reductions of integrals into ones in simpler topologies: (a) one-loop insertion, (b) carpet, (c) triangle and (d) two-loop diamond. A line with a non-integer power is indicated with "$*$". Performing a one-loop insertion integral or carpet integral removes the lines indicated by the arrows. The triangle rule and diamond rule remove one of the lines indicated by the arrows.

2.1. One-loop insertion integral
When a topology contains a massless one-loop insertion graph (figure 2a) as its substructure, one can integrate out the corresponding loop momentum. The integration gives G-functions, which can be expressed in terms of the gamma function and are exact in $D = 4 - 2\epsilon$ space-time dimensions. Graphically the two lines in the loop become a single line but it gets a non-integer power $1/(Q^2)^\epsilon$ of the resultant momentum Q (indicated by "$*$" in figure 2a). The powers of the two propagators can be arbitrary numbers.

2.2. Carpet integral
There is another type of massless one-loop integrals that can be easily performed. When a subgraph is inserted to a one-loop graph (figure 2b), the outer loop can be integrated out first. The powers of the two outer propagators can be arbitrary numbers.

2.3. Triangle rule
When a topology contains a one-loop triangle subgraph depicted in figure 2c, there is a combination of IBP identities that decreases a sum of powers of the three propagators indicated by the arrows (triangle rule). If the powers of the three propagators are positive integers, then recursive use of the triangle rule reduces an integral into a sum of integrals in simpler topologies with one of the three propagators removed. The number of external lines attached to the top

vertex has no restriction. For example, the ladder topology in figure 1a has two triangles where the triangle rule is applicable. Note that non-integer powers of propagators can be introduced by one-loop insertion integrals or carpet integrals and they may disallow a use of the triangle rule.

2.4. Diamond rule

The triangle rule has an extension for multi-loop diamond-shaped subgraphs [40]. Figure 2d shows the simplest diamond structure, which appears at the four-loop level for the first time and removes one of the six lines indicated by the arrows.

2.5. Special rule

In the non-planar topology in figure 1b (referred as "no1" in `Forcer`), one cannot find any of the above substructures. For a topology where none of the useful substructures is available, one has to prepare "manually" solved IBP reduction rules in such a way that integrals are reduced to ones in simpler topologies or at least to the master integral in the topology. We used considerably computer-assisted derivations of IBP reduction rules for each topology, although it has not been fully automatized.

We start from a set S_0 of IBP identities, which are constructed in the usual way,

$$S_0 = \{I_1, \dots, I_{R_0}\}. \tag{1}$$

Each IBP identity, given as $I_i = 0$, is a linear relation of integrals with various indices. Their coefficients contain the regulator ϵ of dimensional regularization and the indices n_j parametrically. The number of the relations is $R_0 = L(L+E)$ for an L-loop topology with E-independent external momenta. We make a set S_1 of relations obtained from S_0 with an index shifted by one in all possible ways. The set S_1 has $R_1 = NR_0$ elements for a topology with N-indices. Many useful reduction rules can be found as a linear combination of IBPs in the combined set of $S_0 \cup S_1$:

$$\sum_i c_i I_i = 0, \qquad I_i \in S_0 \cup S_1. \tag{2}$$

Basically this is achieved by elimination of complicated integrals in the system. We have constructed an reduction scheme for each topology by combining resulted identities.

3. Construction of the reduction flow for all topologies

In the `Mincer` program, all topologies appearing in the problem were classified by their substructure and all the cases, requiring reductions discussed in section 2, were programmed by hand. This means that the program also contains code for transition from a topology to simpler topologies, for example, rewriting a missing momentum that does not exist in a simpler topology and applying topology symmetries that equate several topologies and so on. At the four-loop level, however, it becomes highly complicated and error-prone. Therefore one should completely automatize the code generation for handling each topology and transition among topologies as well as the classification.

We represent a topology as an undirected graph in graph theory. This makes it easy to detect substructure in a graph; the classification can be done just by pattern matchings of connections of vertices and edges. The reason why we use undirected graphs is that all propagators are squared p_i^2 and after integration the result is a function of the square of the external momentum Q^2, so their directions do not matter. Undirected graphs exhibit symmetries for such momentum directions. One tricky point is the fact that we use dot products ($p_i \cdot p_j$ or $p_i \cdot Q$) as irreducible numerators, hence an extra minus sign may have to be compensated when a momentum is flipped. Non-integer powers of propagators are treated by assigning "colors" to edges, which enables us to distinguish different numbers of non-integer powers m_i of $1/(p_i^2)^{n_i+m_i\epsilon}$. Massive propagators may be handled by additional colors of edges although all propagators are massless in our problem.

The reduction flow of all topologies is constructed as follows. Starting from the top-level topologies, we consider all possible ways to remove a line for each topology. Topologies with massless tadpoles are immediately discarded. Some of the generated topologies are indeed identical under graph isomorphism, which is detected by graph algorithms. We keep track of all mappings of momenta in topology transitions, which is necessary for rewriting propagators and irreducible numerators. For each topology, the next action is determined by its substructure. Irreducible numerators are chosen in such a way that they do not interfere with the action. Symmetries in a topology are detected as graph automorphisms, which helps to reduce the number of terms in the calculation. We repeat this procedure until all topologies are reduced into the Born graph, which creates the whole reduction flow of all possible topologies in the problem.

We have implemented this method by using `Python` with a graph library `igraph` [41]. The program generates `FORM` code in the end. From 11 top-level topologies at the four-loop level, 437 non-trivial topologies appear in the reduction flow. The numbers of topologies with one-loop insertions, carpet integrals, triangles and diamonds are 335, 24, 53 and 4, respectively. The remaining 21 topologies require special rules.

4. Discussion

Together with the special rules and a set of auxiliary library routines, the `FORM` code generated as in section 3 leads to the `Forcer` package. To give a feeling about the performance of `Forcer`, we performed a benchmark reduction of $\mathbf{no1}(2,2,2,2,2,2,2,2,2,2,2,-1,-1,-1)$, which is obtained by increasing indices for all propagators and decreasing them for all irreducible numerators from the master integral $\mathbf{no1}(1,1,1,1,1,1,1,1,1,1,1,0,0,0)$ in the "no1" topology (figure 1b). It took about 4 hours on a desktop PC with 4 cores. This can be improved if one uses a truncated expansion of ϵ in intermediate steps rather than rational arithmetic.

In practice, one needs to compute Feynman diagrams, which must be also automatically generated in some way. Our setup uses `QGRAF` [42] for generating diagrams. The output is then manipulated in `FORM`, as discussed in Ref. [43], and passed to `Forcer`.

The correctness of the program was checked by recomputing several known results found in the literature. Especially, an computation of the four-loop QCD beta function [44, 45] via renormalization constants of self-energies and a vertex with keeping the full dependence of the gauge parameter provides a strong check (the final result of the beta function is of course gauge independent in the minimum subtraction scheme). Others include lower moments of the four-loop splitting functions in the flavor non-singlet sector [7, 8, 9, 10].

`Forcer` was successfully used for several calculations. In Refs. [46, 47], Mellin moments of the four-loop splitting functions and coefficient functions were studied. They include the moments of the splitting functions up to $N = 6$ and $N = 4$ for the non-singlet and singlet cases, respectively, and the moments for structure functions $F_{2,ns}$ and $F_{L,ns}$ up to $N = 6$. Interestingly, the full N-dependence of n_f^2 contributions to non-singlet splitting functions and n_f^3 contributions to singlet splitting functions at this order can be completely determined by computing a fairly large number of Mellin moments and using the LLL algorithm [48]. In Ref. [49], by combining `Forcer` with the R^*-operation [50, 51, 52, 53], the five-loop beta function of Yang-Mills theory coupled to fermions for a general gauge group was obtained, which extended and hence confirmed results obtained in Refs. [54, 55]. More physics results by `Forcer` will be reported elsewhere [56].

The construction of the reduction flow described in section 3 is applicable also at the five-loop level. There are 6570 topologies obtained from 64 top-level topologies. However, 284 topologies have no useful substructure and they require special reduction rules. At present, this seems rather difficult and probably it requires complete automatization for solving IBP relations. Furthermore, derivation of parametric reduction rules can be helpful for other processes. Even partial reductions could be used for preprocessing input integrals in other generic IBP solvers, e.g., Laporta's algorithm, and might give a performance gain. We leave these problems for future work.

Acknowledgments
We would like to thank Joshua Davies, Franz Herzog and Andreas Vogt for discussions and collaboration for physics applications. This work is supported by the ERC Advanced Grant no. 320651, "HEPGAME". Figures were drawn with `Axodraw2` [57].

References
[1] Anastasiou C, Duhr C, Dulat F, Furlan E, Gehrmann T, Herzog F, Lazopoulos A and Mistlberger B 2016 *JHEP* **05** 058 (*Preprint* 1602.00695)
[2] Larin S A, van Ritbergen T and Vermaseren J A M 1994 *Nucl. Phys.* **B427** 41–52
[3] Larin S A, Nogueira P, van Ritbergen T and Vermaseren J A M 1997 *Nucl. Phys.* **B492** 338–78 (*Preprint* hep-ph/9605317)
[4] Retey A and Vermaseren J A M 2001 *Nucl. Phys.* **B604** 281–311 (*Preprint* hep-ph/0007294)
[5] Moch S, Vermaseren J A M and Vogt A 2004 *Nucl. Phys.* **B688** 101–34 (*Preprint* hep-ph/0403192)
[6] Vogt A, Moch S and Vermaseren J A M 2004 *Nucl. Phys.* **B691** 129–81 (*Preprint* hep-ph/0404111)
[7] Baikov P A and Chetyrkin K G 2006 *Nucl. Phys. Proc. Suppl.* **160** 76–9
[8] Velizhanin V N 2012 *Nucl. Phys.* **B860** 288–94 (*Preprint* 1112.3954)
[9] Velizhanin V N 2014 *Preprint* 1411.1331
[10] Baikov P A, Chetyrkin K G and Kühn J H 2015 *Nucl. Part. Phys. Proc.* **261-262** 3–18 (*Preprint* 1501.06739)
[11] Baikov P A and Chetyrkin K G 2010 *Nucl. Phys.* **B837** 186–220 (*Preprint* 1004.1153)
[12] Lee R N, Smirnov A V and Smirnov V A 2012 *Nucl. Phys.* **B856** 95–110 (*Preprint* 1108.0732)
[13] Tkachov F V 1981 *Phys. Lett.* **B100** 65–8
[14] Chetyrkin K G and Tkachov F V 1981 *Nucl. Phys.* **B192** 159–204
[15] Bollini C G and Giambiagi J J 1972 *Nuovo Cim.* **B12** 20–6
[16] 't Hooft G and Veltman M J G 1972 *Nucl. Phys.* **B44** 189–213
[17] Laporta S 2000 *Int. J. Mod. Phys.* **A15** 5087–159 (*Preprint* hep-ph/0102033)
[18] Anastasiou C and Lazopoulos A 2004 *JHEP* **07** 046 (*Preprint* hep-ph/0404258)
[19] Smirnov A V 2008 *JHEP* **10** 107 (*Preprint* 0807.3243)
[20] Smirnov A V and Smirnov V A 2013 *Comput. Phys. Commun.* **184** 2820–7 (*Preprint* 1302.5885)
[21] Smirnov A V 2014 *Comput. Phys. Commun.* **189** 182–91 (*Preprint* 1408.2372)
[22] Studerus C 2010 *Comput. Phys. Commun.* **181** 1293–300 (*Preprint* 0912.2546)
[23] von Manteuffel A and Studerus C 2012 *Preprint* 1201.4330
[24] Baikov P A 1996 *Phys. Lett.* **B385** 404–10 (*Preprint* hep-ph/9603267)
[25] Baikov P A 2006 *Phys. Lett.* **B634** 325–9 (*Preprint* hep-ph/0507053)
[26] Lee R N 2012 *Preprint* 1212.2685
[27] Lee R N 2014 *J. Phys. Conf. Ser.* **523** 012059 (*Preprint* 1310.1145)
[28] Tkachov F V 1983 *Theor. Math. Phys.* **56** 866–70
[29] Chetyrkin K G, Kataev A L and Tkachov F V 1980 *Nucl. Phys.* **B174** 345–77
[30] Gorishny S G, Larin S A, Surguladze L R and Tkachov F V 1989 *Comput. Phys. Commun.* **55** 381–408
[31] Strubbe H 1974 *Comput. Phys. Commun.* **8** 1–30
[32] Larin S A, Tkachov F V and Vermaseren J A M The FORM version of MINCER NIKHEF-H/91-18
[33] Vermaseren J A M 2000 *Preprint* math-ph/0010025
[34] Kuipers J, Ueda T, Vermaseren J A M and Vollinga J 2013 *Comput. Phys. Commun.* **184** 1453–67 (*Preprint* 1203.6543)
[35] Velizhanin V N 2012 *Nucl. Phys.* **B864** 113–40 (*Preprint* 1203.1022)
[36] Moch S, Vermaseren J A M and Vogt A 2014 *Nucl. Phys.* **B889** 351–400 (*Preprint* 1409.5131)
[37] Ueda T, Ruijl B and Vermaseren J A M 2016 *J. Phys. Conf. Ser.* **762** 012060 (*Preprint* 1604.08767)
[38] Ueda T, Ruijl B and Vermaseren J A M 2016 *PoS* **LL2016** 070 (*Preprint* 1607.07318)
[39] Ruijl B, Ueda T and Vermaseren J A M in preparation
[40] Ruijl B, Ueda T and Vermaseren J 2015 *Phys. Lett.* **B746** 347–50 (*Preprint* 1504.08258)

[41] Csardi G and Nepusz T The igraph software package for complex network research *InterJournal* **Complex Systems** (2006) 1695, `http://igraph.org`
[42] Nogueira P 1993 *J. Comput. Phys.* **105** 279–89
[43] Herzog F, Ruijl B, Ueda T, Vermaseren J A M and Vogt A 2016 *PoS* **LL2016** 073 (*Preprint* `1608.01834`)
[44] van Ritbergen T, Vermaseren J A M and Larin S A 1997 *Phys. Lett.* **B400** 379–84 (*Preprint* `hep-ph/9701390`)
[45] Czakon M 2005 *Nucl. Phys.* **B710** 485–98 (*Preprint* `hep-ph/0411261`)
[46] Ruijl B, Ueda T, Vermaseren J A M, Davies J and Vogt A 2016 *PoS* **LL2016** 071 (*Preprint* `1605.08408`)
[47] Davies J, Vogt A, Ruijl B, Ueda T and Vermaseren J A M 2017 *Nucl. Phys.* **B915** 335–62 (*Preprint* `1610.07477`)
[48] Lenstra A K, Lenstra H W and Lovász L 1982 *Math. Ann.* **261** 515–34
[49] Herzog F, Ruijl B, Ueda T, Vermaseren J A M and Vogt A 2017 *JHEP* **02** 090 (*Preprint* `1701.01404`)
[50] Chetyrkin K G and Tkachov F V 1982 *Phys. Lett.* **B114** 340–4
[51] Chetyrkin K G and Smirnov V A 1984 *Phys. Lett.* **B144** 419–24
[52] Chetyrkin K G 2017 *Preprint* `1701.08627`
[53] Herzog F and Ruijl B in preparation
[54] Baikov P A, Chetyrkin K G and Kühn J H 2017 *Phys. Rev. Lett.* **118** 082002 (*Preprint* `1606.08659`)
[55] Luthe T, Maier A, Marquard P and Schröder Y 2016 *JHEP* **07** 127 (*Preprint* `1606.08662`)
[56] Ruijl B, Ueda T, Vermaseren J A M and Vogt A in preparation
[57] Collins J C and Vermaseren J A M 2016 *Preprint* `1606.01177`